Shifts in mercury methylation across a peatland chronosequence: From sulfate reduction to methanogenesis and syntrophy

Haiyan Hu[a,b,*,1], Baolin Wang[c,1], Andrea G. Bravo[d], Erik Björn[e], Ulf Skyllberg[f], David Amouroux[g], Emmanuel Tessier[g], Jakob Zopfi[h], Xinbin Feng[a], Kevin Bishop[c], Mats B. Nilsson[f], Stefan Bertilsson[b,c]

[a] State Key Laboratory of Environmental Geochemistry, Institute of Geochemistry, Chinese Academy of Sciences, 550081 Guiyang, China
[b] Department of Ecology and Genetics, Limnology and Science for Life Laboratory, Uppsala University, SE-75236 Uppsala, Sweden
[c] Department of Aquatic Sciences and Assessment, Swedish University of Agricultural Sciences, SE-75007 Uppsala, Sweden
[d] Department of Marine Biology and Oceanography, Institut de Ciències del Mar (ICM-CSIC), Pg Marítim de la Barceloneta 37-49, E08003 Barcelona, Catalunya, Spain
[e] Department of Chemistry, Umeå University, SE-90187 Umeå, Sweden
[f] Department of Forest Ecology and Management, Swedish University of Agricultural Sciences, SE-90183 Umeå, Sweden
[g] CNRS/Univ Pau & Pays Adour/ E2S UPPA, Institut des Sciences Analytiques et de Physicochimie pour l'Environnement et les Materiaux–mira, UMR5254, 64000, Pau, France
[h] Department of Environmental Sciences, Biogeochemistry, University of Basel, CH-4056 Basel, Switzerland

GRAPHICAL ABSTRACT
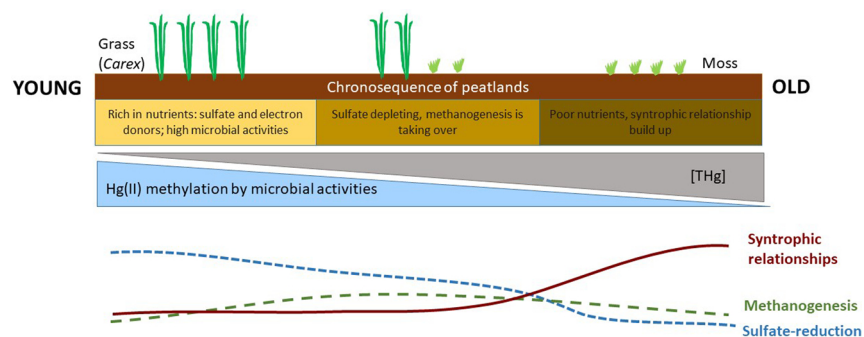
ABSTRACT

Peatlands are globally important ecosystems where inorganic mercury is converted to bioaccumulating and highly toxic methylmercury, resulting in high risks of methylmercury exposure in adjacent aquatic ecosystems. Although biological mercury methylation has been known for decades, there is still a lack of knowledge about the organisms involved in mercury methylation and the drivers controlling their methylating capacity. In order to investigate the metabolisms responsible for mercury methylation and methylmercury degradation as well as the controls of both processes, we studied a chronosequence of boreal peatlands covering fundamentally different biogeochemical conditions. Potential mercury methylation rates decreased with peatland age, being up to 53 times higher in the youngest peatland compared to the oldest. Methylation in young mires was driven by sulfate reduction, while methanogenic and syntrophic metabolisms became more important in older systems.

* Corresponding author at: State Key Laboratory of Environmental Geochemistry, Institute of Geochemistry, Chinese Academy of Sciences, 550081 Guiyang, China.
E-mail address: huhaiyan@mail.gyig.ac.cn (H. Hu).
[1] These authors contribute equally.

Demethylation rates were also highest in young wetlands, with a gradual shift from biotic to abiotic methylmercury degradation along the chronosequence. Our findings reveal how metabolic shifts drive mercury methylation and its ratio to demethylation as peatlands age.

1. Introduction

Mercury (Hg) contamination is an important environmental issue, with methylmercury (MeHg) being the species of most concern due to its toxicity and degree of bioaccumulation in aquatic and terrestrial food webs, with severe negative impacts on wildlife and human health (Clarkson, 1997; Mergler et al., 2007). One of the major routes of human MeHg exposure is consumption of contaminated fish (Mason et al., 2012). This health hazard is mirrored in strict guidelines on fish consumption published for many geographic regions, especially at high latitudes where peatlands are abundant (USEPA, 2017; Becker et al., 2007; Petersson-Grawé et al., 2007; s.o. Michigan, State of Michigan, 2016).

Numerous studies have demonstrated that peatlands are long-term sinks for inorganic Hg, but represent important sources of MeHg to adjacent aquatic ecosystems (StLouis et al., 1996; ; Branfireun and Roulet, 2002; Mitchell et al., 2008; Tjerngren et al., 2012a; Liu et al., 2018; Perez-Rodriguez et al., 2018). In fact, the proportion of peatlands in boreal forest catchments seems to constitute a master control of MeHg loading to downstream aquatic environments (StLouis et al., 1996;). However, peatlands are diverse with respect to hydrology and biogeochemistry and thus the prevailing environmental conditions that control methylation and demethylation processes are highly variable. Nutrient poor peatlands, i.e bogs and nutrient poor fens are low in all weathering derived minerogenic elements while mesotrophic and eutrophic peatlands are defined by high availability of mineral nutrients and other weathering derived elements. Earlier studies have reported that boreal peatlands with intermediate nutrient status seem to be the largest sources of MeHg (Tjerngren et al., 2012a; Poulin et al., 2019), while more nutrient-rich wetlands such as black alder swamps can even be sinks for MeHg because of efficient biotic MeHg demethylation activity (Kronberg et al., 2018, 2012). Also the rapid increase in MeHg net formation caused by artificial (St Louis et al., 2004) and beaver-induced (Selvendiran et al., 2008; Ortega et al., 2018) impoundment of forest soils and wetlands, as well as decline in net MeHg production with aging of these environments are consistent with the idea of wetland trophic status controlling the ratio between rates of Hg(II) methylation and MeHg demethylation (Tjerngren et al., 2012a). This concept finds further support in several studies that point to "poor fen-type" peatlands as hot-spots for MeHg net production and export (StLouis et al., 1996; Tjerngren et al., 2012a). So far, studies have been mainly observational and the specific microbial metabolic pathways driving Hg transformation processes across trophic gradients remain to be explored in a more systematic way.

MeHg formation is mediated by anaerobic organisms carrying hgcA and hgcB genes (Parks et al., 2013), notably by specific lineages of sulfate- (SRB) (Compeau and Bartha, 1985) and iron-reducing bacteria (FeRB) (Fleming et al., 2006), methanogens (Hamelin et al., 2011) and fermenters (Gilmour et al., 2013). Recent studies have shown that Hg(II) methylating communities in wetlands are phylogenetically diverse (Kronberg et al., 2018; Schaefer et al., 2014). Yet, the specific contribution of different microbial functional groups to Hg(II) methylation rates and the detailed understanding of microbial metabolisms controlling Hg(II) methylation in natural ecosystems in general, and in peatlands in particular, are not well understood. To bridge this gap in knowledge, the present study was designed to reveal the metabolic processes responsible for Hg(II) methylation along a trophic gradient in peatland soils.

It is well-known that land uplift along high latitude coastal areas results in ecosystems differing in age up to ~10'000 years within geographically restricted areas with only minor differences in geology and climate (Laine et al., 2018). As a peatland ages after its initiation, peat accumulation disconnects the peatland surface from underlying mineral soils and the supply of weathering products from the mineral soils in the watershed. Therefore the peatland aging leads to an oligotrophication of the peatland (Laine et al., 2018; Tuittila et al., 2013). We therefore hypothesize that the aging-related changes in the trophic status of peatlands will be expressed in the activity and composition of their microbial communities and thus in their potential to form MeHg. To test this, the present study investigates the role of biogeochemical differences for Hg(II) methylation along a peatland chronosequence (0–3200 years) situated in northern Sweden. We conducted controlled laboratory incubation experiments to assess the relative importance of different microbial metabolic processes on Hg(II) methylation and MeHg demethylation. Our work provides a new perspective on Hg(II) methylation across peatlands which can be used to conceptualize our understanding of the dominating ecohydrological and biogeochemical controls on mercury methylation and the MeHg supply to downstream surface waters.

2. Materials and methods

2.1. Study area and samples collection

The studied peatland chronosequence is located east of the community of Sävar (Sweden), within < 10 km of the Baltic Sea coast (Fig. S1). Since the last deglaciation the area is undergoing continuous land uplift due to isostatic rebound. Thus, the initiation age of peatlands can be obtained from the shoreline displacement curve for southern Västerbotten (Renberg and Segerström, 1981). Based on the shoreline displacement curve the mires were grouped as follows: young (< 10 m.a.s.l, < 1000 years), intermediate age (10–20 m.a.s.l, 1000–2000 years) and old (20–40 m.a.s.l, > 2000 years). In this study, we investigated THg and MeHg concentrations in 15 peatlands, with each age group featuring 5 peatlands (Table 1).

Among them, one peatland from each class was selected for microcosm incubation studies, including S02 and S65, the youngest and the oldest mire, respectively, as well as the middle-aged site S16 (Table 2). In Table 2, key geographical information and geochemical

Table 1
Contents of total Hg and MeHg and %MeHg in the investigated peatland chronosequence. The sites S02, S16, and S65 were selected for microcosm incubations, representing the young, intermediate and old peatland, respectively.

Peatland type	Site	Age (year)	THg (ng/g)	MeHg (ng/g)	%MeHg (%)
Young	**S02**	**72**	**33**	**12**	**37**
	S70	149	50	5.0	10
	S43	341	37	1.4	3.7
	S13	352	37	3.4	9.0
	S10	503	25	5.3	21
Intermediate	S52	1221	45	6.7	15
	S14	1341	25	3.7	15
	S18	1401	75	1.9	2.6
	S16	**1402**	**101**	**6.2**	**6.1**
	S62	1495	55	3.5	6.5
Old	S29	2547	47	2.0	4.2
	S26	2686	61	0.9	1.4
	S33	2799	133	5.4	4.0
	S24	2874	67	5.2	7.7
	S65	**3146**	**91**	**2.2**	**2.4**

Table 2
Geochemical characterization of the peatlands selected for the microcosm experiments.

| Site No. | S02 | S16 | S65 |
Peatland type	Young	Intermediate	Old
Age (years)	72	1402	3146
N coordinate	63°51'3.90"	63°52'47.97"	63°52'58.48"
E coordinate	20°42'54.12"	20°42'22.49"	20°38'50.03"
Elevation (m)	0.7	14.6	34.8
pH (n = 5)	4.9 ± 0.27	4.2 ± 0.10	3.9 ± 0.04
Ground water level (cm)[a](n = 5)	15 ± 3.4	13 ± 3.7	12 ± 2.5
Total C (%)	45.1	48.6	49.4
Total N (%)	1.1	1.1	1.3
C/N ratio	42.3	46.3	36.9
Al (mg/g dw)	1.4	2.3	1.3
Ca (mg/g dw)	2.9	2.4	1.2
Fe (mg/g dw)	7.4	4.7	3.3
S (mg/g dw)	3.7	2.0	2.0
P (mg/g dw)	0.81	0.44	0.48
K (mg/g dw)	1.0	0.19	0.21
Na (mg/g dw)	0.80	0.13	0.07
Mg (mg/g dw)	2.4	0.56	0.35
Mn (mg/g dw)	0.030	0.017	0.009
Si (mg/g dw)	3.9	1.5	2.0
Zn (mg/g dw)	0.017	0.018	0.021
Lactate (µM) (n = 3)	15 ± 5.8	6.2 ± 1.6	7.8 ± 2.3
Acetate (µM) (n = 3)	5.3 ± 3.6	10 ± 6.6	4.7 ± 1.9
Propionate (µM) (n = 3)	5.9 ± 0.7	3.1 ± 1.0	3.9 ± 1.2
Butyrate (µM) (n = 3)	7.7 ± 2.2	3.5 ± 0.5	2.1 ± 1.5
Sulfate (µM) (n = 3)	34 ± 8.9	6.4 ± 1.0	5.4 ± 0.4
Sulfide ((µM) (n = 3)	1.11 ± 0.09	0.64 ± 0.07	0.70 ± 0.13
DOC(mg/L) (n = 3)	59.5 ± 2.6	49.6 ± 0.64	54.2 ± 5.9
Chloride (µM) (n = 3)	411 ± 29	75 ± 19	55 ± 8.7

[a] Indicates the growing season average water table. Data with " ± " indicates mean ± SE.

properties of the selected peatlands are summarized. The characteristic plants of the ground and field layer vegetation can be found in Table S1 and Fig. S2. We also compared our peatlands with others from around the world with respect to wetland type, pore water pH, k_m, k_d, %MeHg, as well as concentrations of sulfate, THg and MeHg (Table S2).

Samples were collected in August 2016. Five peat cores were collected from each site with sampling points across the peatland center and at least 5 m away from each other. The upper 10 cm peat soils beneath the annual growing season ground water table were sampled and stored in double polyethylene zip-lock bags. Subsamples were taken for incubation studies and for chemical analyses. After removal of peat samples, the pore water which refilled the holes left by the sampling was collected and stored in borosilicate glass bottles, as soon as the water level stabilized. The peat soils and pore water samples were kept dark and cool on ice during transport until further processing within two weeks.

2.2. Chemical analyses

THg was analyzed by solid combustion atomic absorption spectrometry (DMA-80, Milestone, Italy) using certified marine sediment reference material MESS-3 (National Research Council of Canada, 0.091 ± 0.009 mg Hg kg^{-1}) for calibration. MeHg contents in peatland soils were measured by isotope dilution analysis described in detail elsewhere (Lambertsson et al., 2001). Briefly, the peat soils were extracted using a solution containing $KBr/CuSO_4/H_2SO_4/CH_2Cl_2$. A species-specific isotopically enriched internal standard was added prior to the solid–liquid extraction, followed by ethylation and preconcentration. The preconcentrated sample was analyzed by thermal desorption onto a GC-ICPMS (Agilent 6890 N GC, Agilent 7500 ICPMS, Agilent Technologies, USA). Measurements of other chemical parameters in soils and pore water were described in detail elsewhere (Tjerngren et al., 2012b).

2.3. Microcosm incubation experiments

The peat soil and pore water were homogenized to make slurries in a 2-L beaker by gentle blending (Philips HR hand blender) in a glove box under N_2 atmosphere. Water content was adjusted to approximately 95 % (wt/wt), which was determined as weight loss after drying at 60 °C until constant weight. The slurries (30 mL) were dispensed into 120 mL serum bottles and sealed with butyl rubber septa and aluminum crimp caps. In order to remove residual oxygen, the slurries were preincubated in the dark at 18 °C for 14 days. Thereafter, the bottles were supplemented with different combinations of SO_4^{2-}, MoO_4^{2-}, BES (2-bromoethanesulphonate), FeOOH and/or organic acids (lactate, propionate and butyrate) (Table 3), followed by a spike with stable Hg isotope tracer, as described below. Two types of control incubations were included: sterile controls with autoclaved (121 °C for 30 min) peat soil; and reference controls with original peat soil, but without any additions of inhibitors or any treatment (Table 3).

All reagents used in the incubation experiments were prepared using oxygen-free Millipore water as described elsewhere (Hu et al., 2013; Bravo et al., 2015) and all the processes involved in sediment handling and treatments were carried out in a N_2-filled glove box in order to prevent oxidation of reduced chemical species or inactivation of anaerobic microorganisms (Bravo et al., 2015).

2.4. Determination of potential methylation (k_m) and demethylation (k_d) rates

After the addition of the supplements, slurries were spiked with isotopically enriched $^{204}HgCl_2$ (98.11 %) and $Me^{200}HgCl$ (96.41 %) at concentrations similar to ambient values (Table 1). The enriched Hg isotopes were purchased from Oak Ridge National Laboratory (TN,

Table 3
Specific inhibitors and stimulators used in the microcosm experiments and their expected effects.

No.	ID	Manipulations		Expected effects
		Substance	Conc. (mM)	
1	Mo	Na_2MoO_4	1	Inhibit sulfate-reduction and SRB that grow as fermenters
2	BES	2-bromoethanesulphonate	5	Inhibit methanogenesis and syntrophy
3	MoBES	Na_2MoO_4 + BES	1 + 5	Inhibit sulfate-reduction, methanogenesis and syntrophy
4	SO_4^{2-}	Na_2SO_4	1	Stimulate sulfate-reduction
5	Fe	FeOOH	1	Stimulate iron-reduction
6	LBP	lac + but + pro	1 + 1 + 1	Stimulate syntrophy and methanogenesis
7	LBPMo	lac + but + pro + Na_2MoO_4	1 + 1+1 + 1	Stimulate syntrophy and methanogenesis but inhibit sulfate-reduction
8	LBPBES	lac + but + pro + BES	1 + 1+1 + 5	Inhibit methanogenesis
9	LBPSO4	lac + but + pro + Na_2SO_4	1 + 1+1 + 1	Stimulate sulfate-reduction and syntrophy
10	Reference control	No treatment	Original peats	Original states
11	Sterile control	autoclaved	121 °C, 30 min	Abiotic processes

lac: sodium lactate; but: sodium butyrate; pro: sodium propionate.

USA), and the MeHg tracer was synthesized as described by Jonsson et al (Jonsson et al., 2012). The "T0″ sample was collected within 5 min after tracer amendment. Part of the slurry was frozen at −80 °C for later determination of Hg(II) methylation and MeHg demethylation rates. The rest of the slurry was centrifuged at 3100 × g and 4 °C for 10 min to collect the pore water. Pore water was sequentially filtered through a 0.45 μm Millex®-HV PVDF filter (Millex, cat No. SLHV033RK) and a 0.22 μm cyclopore track etched membrane filter (Whatman, cat No. 7063-2502), for the analysis of chemical parameters. For each treatment, three peat soil replicates were spiked with $^{204}HgCl_2$ and $Me^{200}HgCl$ and incubated for 24 h in the glove box at 18 °C, corresponding roughly to the peat temperature in summer. At the end of any incubation, a similar sampling protocol as for T0 was used to collect pore water and solid phases for chemical analyses.

Hg(II) and MeHg were extracted from 200 mg of wet slurries using 7 mL of 6 N HNO_3 (J.T. Baker, CAS No.7697-37-2) and focused microwave treatment at 75 °C for 4 min. Remaining particles were subsequently removed by centrifugation. The extracts were analyzed by species-specific isotope dilution and capillary gas chromatography (Trace GC Ultra, Thermo Fisher, Waltham, MA, USA equipped with a TriPlus RSH autosampler) hyphenated to an inductively coupled plasma mass spectrometer (Thermo Scientific, XSeries 2 ICP-MS) to correct for species inter-conversion (Rodriguez-Gonzalez et al., 2013; Martin-Doimeadios et al., 2003). Briefly, the extracts were buffered at pH 4 and isotopic-enriched Hg species $^{199}Hg(II)$ and $Me^{201}Hg$ were then added for quantification. The different Hg species were then ethylated with sodium tetraethyl borate and recovered in isooctane. Each sample was analyzed three times, and blank extractions were included to check for contamination. The concentrations of recovered Hg species carrying the added isotopes ($Me^{200}Hg$, $^{200}Hg(II)$, $Me^{204}Hg$, $^{204}Hg(II)$) and methylation/demethylation yields were calculated by isotopic pattern deconvolution methodology using known concentrations and abundances of $Me^{201}Hg$ and $^{199}Hg(II)$ (Rodriguez-Gonzalez et al., 2013). The measurement error (calculated by analyzing each sample three times) was usually less than 7 % for Hg(II) and MeHg concentrations. The measured values were within the certified range for all analyses, with a 92 ± 1 % (n = 3) recovery of THg of the certified reference material (IAEA-405).

2.5. Calculation of contributions of different microbial metabolism pathways to Hg(II) methylation

In order to calculate the relative contributions of different metabolisms to Hg(II) methylation, we inhibited sulfate reduction and methanogenesis by amending Mo and BES, respectively. The syntrophic metabolism between SRB fermenters and methanogens was inhibited by

Mo and/or BES. Based on the inhibition of k_m from exposure to Mo, BES and MoBES, and assuming that the contribution from the different groups is additive, we calculated the relative contributions to Hg(II) methylation from different microbial metabolic processes, including sulfate-reduction, methanogenesis, and syntrophic metabolism between methanogens and SRB that grow as fermenters. The relative contributions of different microbial metabolisms to Hg(II) methylation was calculated by the differences of k_m between the treatments of specific microbial inhibitors and the control, using Eqs. (1), (2) and (3).

$$k_m\_Mo = k_m\_control – k_m\_SR – k_m\_Syn \qquad (1)$$

$$k_m\_BES = k_m\_control – k_m\_Meth – k_m\_Syn \qquad (2)$$

$$k_m\_MoBES = k_m\_control – k_m\_SR – k_m\_Meth – k_m\_Syn \qquad (3)$$

k_m_Mo, k_m_BES, k_m_MoBES refer to the k_m in the treatment of Mo, BES and MoBES, respectively; $k_m\_control$ refers to the k_m in the control incubations; k_m_SR, k_m_Meth, k_m_Syn refer to the k_m contributed by sulfate reduction, methanogenesis, and syntrophic metabolism between methanogens and SRB fermenters, respectively.

This calculation was based on the following documented principles: (1) Mo broadly inhibits SRB, not only those engaging in dissimilatory SO_4^{2-} respiration but also those thriving by fermentation in a syntrophic relationship with methanogens (Taylor and Oremland, 1979; Wu et al., 1991). This implies that inhibition of k_m by Mo covers both pathways, Hg methylation by respiring as well as fermenting SRB (Bae et al., 2014) (Fig. 1). (2) Likewise, BES inhibits methanogenesis (Zehnder and Brock, 1979), but it also affects syntrophic interactions (Fig. 1). Firstly, upon BES addition, the activity of the syntrophic fermenters is inhibited (thermodynamically) by increasing H_2 concentration; Secondly, the inhibition of methanogens by BES interrupts direct electron transfer (DIET) between syntrophic fermenters and the electron accepting methanogens (Rotaru et al., 2014; Walker et al., 2018); (3) A combination of Mo and BES (MoBES) inhibits all of sulfate reduction, methanogenesis and the syntrophic metabolism between both partners. The difference between MoBES and the control was considered as the contribution from other microbial metabolisms, such as iron reduction, regular fermentation, and non-SRB syntrophs.

2.6. Statistical analyses

IBM SPSS Statistics 24 (SPSS Inc., USA) was used for statistical analyses. All data were checked for normality and homoscedasticity, using Shapiro-Wilkinson and Levene's tests, respectively. Non-normally distributed data were log transformed before undergoing statistical tests. Significant differences in k_m and k_d among sites and treatments were tested by one-way ANOVA (analysis of variance, $p = 0.05$),
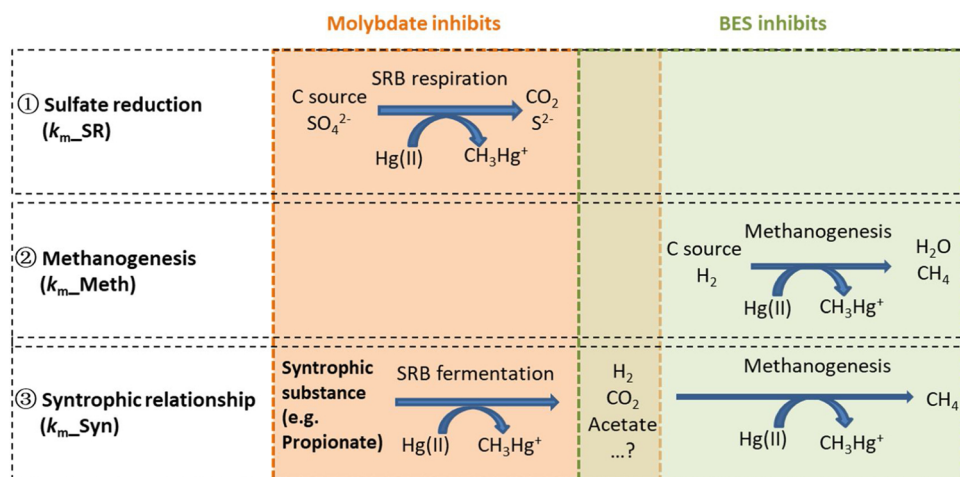

Fig. 1. Conceptual figure showing the effects of different inhibitors on microbial metabolisms and Hg(II) methylation rates. In pathway ③, the metabolites from SRB fermentation provides substrate for methanogensis, i.e. H_2, CO_2, acetate and other uncertain metabolites exchange, while methanogenesis makes the former reaction continue by consuming H_2. Molybdate amendments inhibit ① and ③, whereas BES amendments inhibit ② and ③. Amendments of both molybdate and BES, inhibit ① ② and ③. k_m_SR, k_m_Meth, k_m_Syn represent the contributions of corresponding pathways to k_m.

followed by Tukey's HSD post hoc analysis ($p = 0.05$) to identify statistically differing groups.

3. Results and discussion

3.1. High Hg(II) methylation in young peatlands

The three age classes of 15 peatlands exhibited different biogeochemical characteristics in superficial peat (0–10 cm depth) along the chronosequence with respect to THg, MeHg and %MeHg (Tables 1 and 2). The concentrations of THg expressed in relation to peat dry mass were significantly higher ($p = 0.023$) in old peatlands (Table 1). Both the absolute concentrations (ng/g dw) and the relative (% of THg) concentrations of MeHg were highest in the young peatlands (Table 1). The MeHg levels were within the range of concentrations reported from other boreal wetland soils (Tjerngren et al., 2012b; Liu et al., 2003; Warner et al., 2003; Skyllberg et al., 2003), while MeHg concentration in the youngest peatland was at the higher end of previous observations. %MeHg in the youngest peatland was also among the highest reported for boreal wetlands, whereas the intermediate and older peatlands agreed with previous observations in Swedish peatlands (Tjerngren et al., 2012b; Skyllberg et al., 2003). From an international perspective, %MeHg observed in the intermediate and old peatlands were still higher than reported for many other wetlands, *i.e.* a Chinese bog (Liu et al., 2003), Canadian High Arctic wetlands (Loseto et al., 2004) and cattail wetlands in California, USA (Table S2).

To specifically investigate the relative contributions from different microbial metabolisms (*i.e.* sulfate reduction, methanogenesis and syntrophic interaction) to Hg(II) methylation and demethylation processes, we selected two end-members and one peatland of intermediate age to experimentally determine Hg(II) methylation (k_m) and MeHg degradation (k_d) rate constants in soil samples amended with specific microbial inhibitors, electron donors and electron acceptors (Table 3). Results showed that the young peatland presented a much higher k_m than the intermediate ($p = 0.017$) and old systems ($p = 0.016$) (Fig. 2a). The measured k_m in the young peatland was either higher or at the high end of reported values for boreal wetlands and sediments (Tjerngren et al., 2012b; Lehnherr et al., 2012) (Table S2). In contrast, the k_m in the intermediate and old peatlands was at the lower end of this spectrum. Similar to k_m, the MeHg demethylation rate constant, k_d, was higher in the young peatland compared to intermediate ($p = 0.004$) and old ones ($p = 0.003$) (Fig. 2a). Therefore, in comparison to the old ones, both methylation and demethylation processes were enhanced in the young system. While k_m was 26 and 53 times higher in the young peatland compared to the intermediate and old, respectively, k_d was only 2.4 times higher in young as compared to the intermediate and old peatlands.

Because the average concentration of the potent Hg and MeHg complexing ligands sulfide and DOC did not differ among the three sites (Table 2), we do not expect differences in k_m and k_d among sites to be caused by different availability of the added tracers ^{204}HgCl and Me^{200}HgCl in the incubation experiments.

While %MeHg is usually regarded as a good proxy for long-term *in situ* net production of MeHg (Mitchell et al., 2008; Tjerngren et al., 2012b; Lambertsson and Nilsson, 2006; Drott et al., 2008; Benoit et al., 2003), the ratio of k_m/k_d is considered to reflect short-term net MeHg production (Martin-Doimeadios et al., 2004; Bouchet et al., 2013). Trends in %MeHg and k_m/k_d were coupled along the chronosequence (Fig. 2b), indicating a good agreement between long-term *in situ* net MeHg production (%MeHg) and short-term Hg(II) methylation and MeHg demethylation (k_m/k_d ratio). Higher %MeHg and k_m/k_d (Fig. 2 and S3) in the young peatland compared to the intermediate and old peatlands suggests that conditions in the young peatland favor methylation more than demethylation, resulting in high MeHg concentrations in young peatlands.

3.2. Sulfate-reduction drives Hg(II) methylation in the young peatland

By performing controlled laboratory incubation experiments, major microbial metabolisms responsible for Hg(II) methylation in peatlands of different chronosequence trophic status and biogeochemistry can be identified (Fig. 1). One common approach to identify Hg(II) methylating guilds and quantify their contributions to Hg(II) methylation rates is the use of specific microbial inhibitors, in particular molybdate and BES to detect the activities of SRB and methanogens, respectively (Fleming et al., 2006; Bae et al., 2014; Yu et al., 2012). As a result, mutualistic interactions between SRB and methanogens, here defined as "syntrophy", have so far been overlooked, as such processes could be inhibited by either molybdate or BES alone or in combination (Fig. 1). The classical definitions of syntrophy emphasize a metabolic cooperation where two or more different organisms are able to catabolize a substrate that neither can access by themselves (Morris et al., 2013; Madigan et al., 2015). In this study, we define syntrophy more broadly, as a mutualistic interaction between on the one hand SRB that grow as fermenters and on the other hand methanogens, where both partners depend on each other to activate or enhance Hg(II) methylation. This definition of syntrophy includes both metabolic interdependencies where Hg(II) methylation is carried out or enhanced by merely one of the partners, or cases where several methylators rely on such mutualistic interactions (Yu et al., 2018; Pak and Bartha, 1998) (Fig. 1).

In our incubation experiments and in line with previous studies (Fleming et al., 2006; Martin-Doimeadios et al., 2004), Hg(II) methylation was almost completely ($k_m < 0.0002$ d^{-1}) absent in sterile controls (referred to as autoclaved) from all studied peatlands (Fig. 3), illustrating that Hg(II) methylation is essentially a biological process. However, the effect of the specific inhibitors and substrates on Hg(II) methylation changed along the peatland chronosequence. In the young peatland, Hg(II) methylation was largely reduced (~ 70 %, $p = 0.007$) by inhibiting sulfate-reduction through the addition of molybdate (referred to as Mo) (Fig. 3a). In contrast, BES that inhibits methanogenesis,
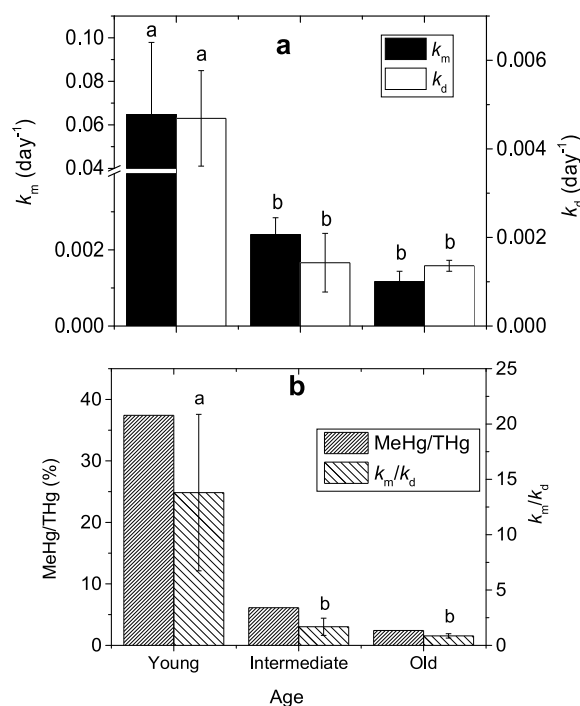

Fig. 2. (a) Hg(II) methylation (k_m) and MeHg demethylation (k_d) rate constants, and (b) %MeHg and k_m/k_d in the chronosequence peatlands. Error bars represent one standard error of the replicate samples from sacrificial incubation bottles (n = 3). Means with the same letter are not significantly different from each other ($p = 0.05$).
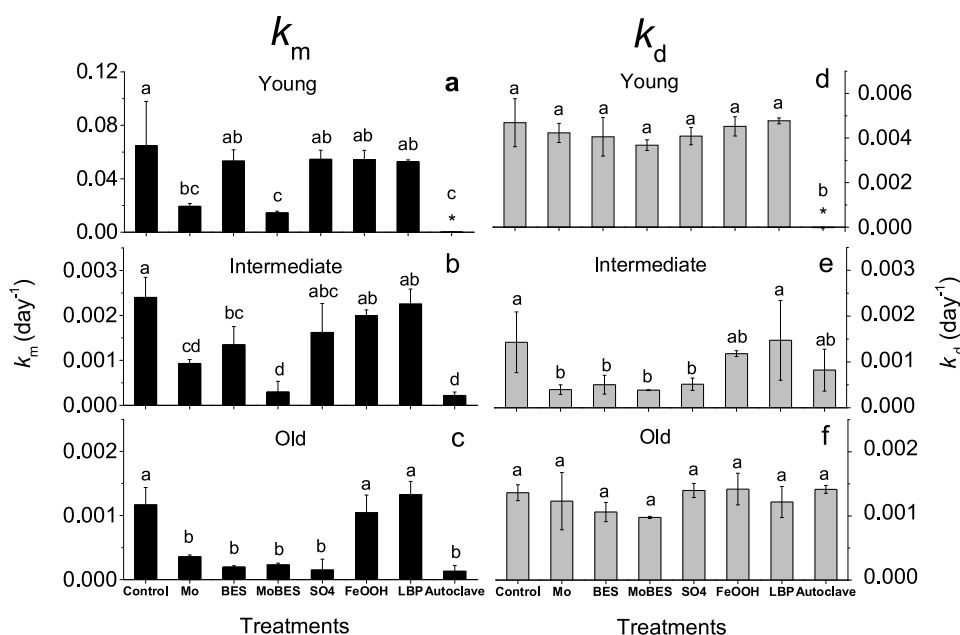
Fig. 3. Hg(II) methylation (k_m) (left) and MeHg demethylation (k_d) (right) rate constants in the different manipulations of the microcosms from the chronosequence of peatlands. Error bars represent one standard error of the replicate samples from sacrificial incubation bottles (n = 3). LBP = sodium lactate (1 mM) + sodium butyrate (1 mM) + sodium propionate (1 mM), Mo = Na_2MoO_4 (1 mM), BES = sodium 2-bromoethanesulphonate (5 mM), SO_4^{2-} = Na_2SO_4 (1 mM). Autoclave (121 °C, 30 min). * indicates the data was too low thus invisible in the figure. Means with the same letter are not significantly different from each other ($p = 0.05$).

had an insignificant effect on k_m ($p = 0.981$) in samples from the young peatland. Adding lactate, butyrate and propionate (referred to as LBP) as electron donors in combination with Mo or BES (Table 3) gave consistent effects, thus LBPMo inhibited k_m significantly ($p = 0.028$) while LBPBES had no significant effect ($p = 0.206$) compared to LBP alone (Fig. S4a). The inhibition effect by Mo alone was similar to the combined treatment Mo + BES (MoBES) (Fig. 3a), suggesting that in young peatlands sulfate reducing microorganisms were responsible for most of the Hg(II) methylation and that their Hg(II) methylating activity was not influenced by the activity of methanogens.

Based on the k_m changes created by different inhibitors (Fig. 3), we calculated (Section 2.5: Eqs. (1)–(3)) the relative contribution of sulfate reduction, methanogenesis, syntrophy and other possible microbial metabolisms to k_m (Fig. 4, Young). Results showed that in the young peatland SRB contributed 70 % of the k_m, of which 60 % was from sulfate reduction and 10 % was from syntrophic interactions between methanogens and SRB that grew as fermenters (Fig. 4, Table S3). Sulfate addition had little effect ($p = 0.992$) on k_m (Fig. 3a), demonstrating that sulfate was not a limiting factor in the young peatland, probably because pore water sulfate concentration in the young peatland (34 ± 8.9 μM; Table 2) was quite high compared to the range reported for Swedish boreal wetlands (5.6 − 17 μM) (Tjerngren et al., 2012b). Similar to sulfate, Fe(III) was likely not a limiting factor in the young peatland, as indicated by the insignificant effects of FeOOH

amendments on k_m ($p = 0.991$). Because there is no specific inhibitor for microbial iron-reduction, we could not robustly quantify the specific contribution of iron-reduction to k_m. However, we indirectly estimated that approximately 22 % of k_m could be attributed to metabolisms other than sulfate-reduction, methanogenesis and syntrophic interactions (Fig. 4). Most likely this is due to the activity of iron-reducers (Fleming et al., 2006; Bravo et al., 2018). The LBP treatment did not have a strong impact on k_m in the young peatland ($p = 0.974$; Fig. 3a), indicating that electron donors for Hg(II) methylators were already readily available in this system. In summary, our results demonstrate that the high MeHg concentrations in young peatlands are caused by high *in situ* MeHg formation, and that sulfate reduction is the main metabolism responsible for this process.

3.3. Peatland aging: under oligotrophic conditions methanogenesis and syntrophy take over

In the intermediate peatland, both Mo (inhibition ≈ 61 %, $p = 0.002$) and BES (inhibition ≈ 44 %, $p = 0.035$) significantly reduced k_m during the incubation. The inhibition was even greater when amendments were applied in combination (MoBES inhibition ≈ 88 %), than for either of the two amendments alone (Fig. 3b, Table S3). This suggests that both SRB and methanogens contributed to k_m at the intermediate site, but that they likely operated independently, *i.e.* there
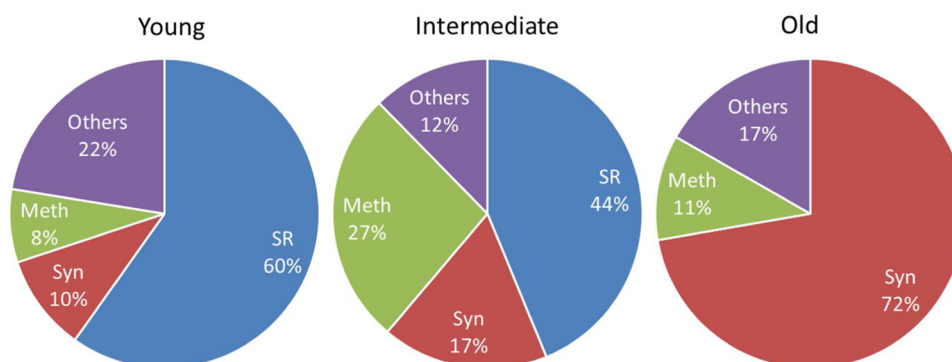

Fig. 4. Relative contributions of different microbial metabolisms to k_m across the peatland chronosequence. SR: sulfate reduction; Meth: methanogenesis; Syn: syntrophic interactions. Others: iron reduction, regular fermentation and other metabolisms like syntrophic fermentation by non-SRB.

was only limited (17 %) syntrophy (Fig. 4).

In the old peatland, k_m was significantly inhibited by both Mo (≈ 69 %, $p = 0.001$) and BES (83 %, $p < 0.001$) (Fig. 3c, Table S3). Because the combination of the two inhibitors had a similar effect as either inhibitor added alone (Fig. 3c), we suggest mutualistic effects between SRB and methanogens (Fig. 4). These most likely involved fermenting SRB stimulating Hg(II) methylation as described above. Indeed, our calculations showed that 83 % of k_m in the old peatland was associated with methanogens, of which 72 % was indicated to represent syntrophic interactions with SRB fermentation (Fig. 3). In contrast, calculations showed that all of the MeHg produced by SRB was attributed to syntrophic metabolism associated with methanogenesis. Unlike the insignificant effects of sulfate on k_m in the young ($p = 0.992$) and intermediate ($p = 0.338$) peatlands, sulfate addition significantly inhibited k_m in the old peatlands ($p < 0.001$) (Fig. 3), further supporting a minor contribution of sulfate reduction to Hg(II) methylation in aged peatlands. If k_m was due to syntrophy, a decrease in k_m in sulfate amended treatments could be explained by a boost of non Hg(II) methylating sulfate reduction metabolism, which might have outcompeted fermenting SRB capable of Hg(II) methylation. Another explanation was that Hg availability for methylation decreased due to the formation of Hg_2S. Further studies are required to answer this question.

Our novel findings reveal that the contribution of sulfate reduction to k_m decreased with decreasing trophic status of the peatlands, while the contribution from syntrophic SRB fermentation and methanogenesis increased. Recent work in the Florida Everglades has shown that syntrophy can be important for Hg(II) methylation (Bae et al., 2014, 2015) and laboratory experiments have demonstrated this also for iron- and sulfate-limited peatlands (Yu et al., 2018).

3.4. Abiotic MeHg demethylation overtakes biotic demethylation with peatland aging

Values for k_d in the different treatments varied among the three peatlands. In the young peatland, k_d was completely inhibited by autoclaving ($p < 0.001$; Fig. 3d), indicating that MeHg demethylation was mainly caused by biotic processes (Oremland et al., 1991). Except for autoclaving, there was no significant difference ($p = 0.842$; Fig. 3) in k_d among the rest of the treatments in the young peatland, suggesting that MeHg demethylation was likely carried out by microorganisms that did not respond to our experimental treatments. In the old peatland, none of the amendments or autoclaving had any significant effect on k_d ($p = 0.737$, Fig. 3f), indicating that abiotic processes dominate MeHg demethylation in the old peatland (Martin-Doimeadios et al., 2004; Hammerschmidt and Fitzgerald, 2006). Unlike the young and old peatlands, k_d was significantly inhibited by Mo ($p = 0.025$), BES ($p = 0.043$), MoBES ($p = 0.024$) and sulfate ($p = 0.037$) in the intermediate peatland (Fig. 3e). Furthermore, k_d in the sterile control was lower than the reference control (Fig. 3e), although the difference was not statistically significant ($p = 0.145$). This suggests that both biotic processes and abiotic processes are likely involved in MeHg degradation in the intermediate peatland. Rates of MeHg demethylation were significantly higher in the youngest wetlands. Yet, in agreement with previous studies, net MeHg production and MeHg pools in most wetlands are largely driven by varying and high Hg(II) methylation rates with only a minor influence from demethylation reactions (Drott et al., 2008; Hammerschmidt and Fitzgerald, 2006). This is because MeHg demethylation rates, even if they are significant and often higher in absolute numbers, generally vary less among different environments, even though the seasonal variability may sometimes be high for demethylation (Kronberg et al., 2012; Martin-Doimeadios et al., 2003). One clear exception is alder swamps, in which a combination of biotic and abiotic processes resulted in a net degradation of MeHg (Kronberg et al., 2018, 2012).

3.5. Environmental implications

In this study, we showed that Hg(II) methylation rates decreased with decreasing trophic status of these peatland ecosystems and that the microbial metabolism dominating Hg methylation changed along this chronosequence of peatlands. These new findings contribute to a better understanding of the variability in MeHg formation across biogeochemical gradients and will help us identify the wetlands posing the highest risk for net formation and export of MeHg to adjacent aquatic ecosystems.

Based on our results and preceding work (Compeau and Bartha, 1985; Hamelin et al., 2011; Liu et al., 2003; Loseto et al., 2004), we propose a conceptual model explaining how Hg(II) methylation pathways shift across the chronosequence of peatlands due to the variability in nutrient concentrations which in turn dictates plant composition and peatlandfunctioning (as shown in the graphical abstract). The high Hg(II) methylation rates in young peatlands can be explained by high pH, low Eh, high availability of nutrients, organic electron donors and electron acceptors (Yu et al., 2012; Morris et al., 2013; Yu et al., 2018), all of which typically decline as peatlands age and become disconnected from the mineral soils both beneath the growing peat and in the surrounding catchment area. Previous studies (StLouis et al., 1996; Mitchell et al., 2008; Tjerngren et al., 2012a; Selvendiran et al., 2008) reported a maximum net MeHg production occurring in the intermediate nutrient category (rich/poor fen) of wetlands. According to the concept of Tjerngren et al. (2012a), the ratio between methylation and demethylation rates is particularly high in these environments. The ratio is suggested to be lower in nutrient poor, low pH peatlands as well as in richer wetlands having more nutrients and higher pH (Fig. 5). In this context, the youngest/most nutrient rich peatland in the present study falls in the intermediate nutrient category. The decrease in nutrient status and pH from intermediate (young) to low levels (old) reduces the ratio between methylation and demethylation, causing a decrease in net MeHg production with increasing peatland age across the chronosequence. Since the absolute rates of demethylation were significantly higher in the young peatland, it is mainly the changes in methylation that drives the observed changes in net Hg methylation. This agrees with the concept that rates of both methylation and demethylation increase with increasing trophic status although the former changes more and reaches its maximum already at intermediate trophic status (Fig. 5).

The changes in peatland chemistry and vegetation composition along the peatland chronosequence also manifest themselves in a shift
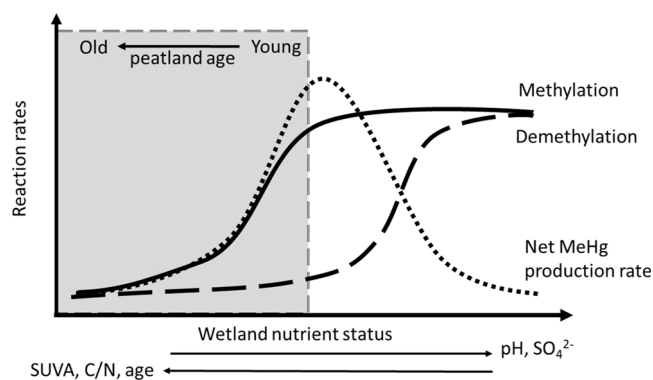

Fig. 5. Hypothesized concept relating methylation, demethylation and net MeHg production rates to nutrient status, where intermediate nutrient category wetlands exhibit maximum net MeHg production as compared to very rich and poor wetlands. Even the richest/youngest peatland of this study is in the poor-to-intermediate nutrient range (left part of the graph) where methylation, demethylation and net MeHg production rates increase with nutrient status. SUVA: specific UV-absorbance at 254 nm.
Adapted from Tjerngren et al. (2012).

of microbial metabolisms responsible for Hg(II) methylation. Our findings suggest that when moving from intermediate to poorer trophic status, syntrophic interaction takes over from sulfate reduction and methanogenesis to dominate Hg(II) methylation (Figs. 4 and 5). Although, the potential importance of syntrophy for Hg(II) methylation in natural ecosystems has already been proposed based on abundance of *hgc*A sequences from *Syntrophobacterales* (Bae et al., 2014), and by co-culturing experiments with two syntrophic partners (Yu et al., 2018; Pak and Bartha, 1998), the present study is, to the best of our knowledge, the first one demonstrating that syntrophic Hg(II) methylation can be quantitatively important in natural ecosystems. In fact, we may well have underestimated the role of syntrophy for Hg(II) methylation, as our experimental approach only enabled us to specifically target syntrophic partnerships between fermentative SRB and methanogens. Other syntrophic partnerships may thus have been overlooked.

Although anthropogenic Hg emissions are expected to decline as a result of the recently implemented UNEP Minamata treaty (UNEP, 2017), many questions remain about how fast environments may recover as a consequence of reduced atmospheric Hg deposition and whether other changes (for example, climate and land use) influence the recovery from Hg pollution. Our observations of high Hg(II) methylation rates and high %MeHg in newly formed peatlands with relatively high trophic status suggest that aquatic systems receiving water from such peatlands will probably have the slowest decline in MeHg bioaccumulation. This may be particularly severe as young peatlands also commonly have high connectivity to surface waters. When the peatlands age and trophic status gradually becomes less favorable for net methylation, Hg(II) methylation is sustained, albeit at lower net rates, by syntrophic Hg(II) methylators. As a consequence, net MeHg formation is likely to persist over thousands of years of peatland development. Moreover, future climate change scenarios predict warmer temperatures, shorter ice- and snow-covered periods and therefore longer periods of water saturated soils, which are prone to MeHg formation while also enhancing the hydrological connectivity between the peatlands and the aquatic network. MeHg formed in peatlands and transported to the aquatic network might be bioaccumulated and biomagnified to aquatic food webs, and thus increase human exposure to Hg, through fish consumption. This is of special concern for the populations relying their diet on fish.

4. Conclusions

Based on the results, the following conclusions can be drawn:

(1) Hg(II) methylation rates varied across the peatland chronosequence trophic gradient, with the younger peatland having higher mercury methylation rate constants.
(2) The major microbial metabolisms driving methylation change completely across the peatland chronosequence trophic gradient. In the young peatland Hg(II) methylation is dominated by sulfate reduction which contributed $\approx$ 60 % of k_m. Methanogensis became more important with decreasing nutrient availability as the peatlands aged until finally Hg(II) methylation by syntrophs dominated, contributing ≈ 72 % to k_m in the oldest, most nutrient poor peatland.
(3) Demethylation rates were higher in younger peatlands, and there was a shift from biotic to abiotic degradation along the chronosequence trophic gradient.

Author contributions

H. Hu, B. Wang, A. G. Bravo, E. Björn, U. Skyllberg, K. Bishop, M. B. Nilsson, and S. Bertilsson identified and designed the sampling of the chronosequence of peatlands. H. Hu, B. Wang, A. G. Bravo and S. Bertilsson conceived the laboratory experiments. B. Wang and A. G. Bravo conducted the sampling campaigns. H. Hu and B. Wang

performed laboratory incubations and chemical analysis. A. G. Bravo and E. Tessier performed the GC-ICPMS analyses of Hg. H. Hu conducted all data treatment, statistical analyses, built the figures and wrote the manuscript with significant assistance and comments from B. Wang, A. G. Bravo, E. Björn, U. Skyllberg, K. Bishop, J. Zopfi, D. Amouroux, M. B. Nilsson, and S. Bertilsson.

Declaration of Competing Interest

The authors declare that they have no known competing financial interests or personal relationships that could have appeared to influence the work reported in this paper.

Acknowledgements

Appendix A. Supplementary data

Supplementary material related to this article can be found, in the online version, at doi:https://doi.org/10.1016/j.jhazmat.2019.121967.

References

Bae, H.S., Dierberg, F.E., Ogram, A., 2014. Syntrophs dominate sequences associated with the mercury methylation-related gene *hgc*A in the water conservation areas of the Florida Everglades. Appl. Environ. Microbiol. 80, 6517–6526.

Bae, H.S., Holmes, M.E., Chanton, J.P., Reddy, K.R., Ogram, A., 2015. Distribution, activities, and interactions of methanogens and sulfate-reducing prokaryotes in the Florida Everglades. Appl. Environ. Microbiol. 81, 7431–7442.

Becker, W., D. PO, P.-G. K, 2007. Risks and Benefits of Fish Consumption, Slv Rapport 12. Swedish national food agency. http://www.slv.se/,2019.

Benoit, J.M., Gilmour, C.C., Heyes, A., Mason, R.P., M. CL, 2003. Geochemical and Biological Controls Over Methylmercury Production and Degradation in Aquatic Ecosystems. American Chemical Society.

Bouchet, S., Rodriguez-Gonzalez, P., Bridou, R., Monperrus, M., Tessier, E., Anschutz, P., Guyoneaud, R., Amouroux, D., 2013. Investigations into the differential reactivity of endogenous and exogenous mercury species in coastal sediments. Environ. Sci. Pollut. R. 20, 1292–1301.

Branfireun, B.A., Roulet, N.T., 2002. Controls on the fate and transport of methylmercury in a boreal headwater catchment, northwestern Ontario, Canada. Hydrol. Earth Syst. Sci. 6, 783–794.

Bravo, A.G., Bouchet, S., Guedron, S., Amouroux, D., Dominik, J., Zopfi, J., 2015. High methylmercury production under ferruginous conditions in sediments impacted by sewage treatment plant discharges. Water Res. 80, 245–255.

Bravo, A.G., Zopfi, J., Buck, M., Xu, J.Y., Bertilsson, S., Schaefer, J.K., Pote, J., Cosio, C., 2018. *Geobacteraceae* are important members of mercury-methylating microbial communities of sediments impacted by waste water releases. ISME J. 12, 802–812.

Clarkson, T.W., 1997. The toxicology of mercury. Crit. Rev. Cl Lab. Sci. 34, 369–403.

Compeau, G.C., Bartha, R., 1985. Sulfate-reducing bacteria - principal methylators of mercury in anoxic estuarine sediment. Appl. Environ. Microbiol. 50, 498–502.

Drott, A., Lambertsson, L., Bjorn, E., Skyllberg, U., 2008. Do potential methylation rates reflect accumulated methyl mercury in contaminated sediments? Environ. Sci. Technol. 42, 153–158.

Fleming, E.J., Mack, E.E., Green, P.G., Nelson, D.C., 2006. Mercury methylation from unexpected sources: molybdate-inhibited freshwater sediments and an iron-reducing bacterium. Appl. Environ. Microbiol. 72, 457–464.

Gilmour, C.C., Podar, M., Bullock, A.L., Graham, A.M., Brown, S.D., Somenahally, A.C., Johs, A., Hurt, R.A., Bailey, K.L., Elias, D.A., 2013. Mercury methylation by novel microorganisms from new environments. Environ. Sci. Technol. 47, 11810–11820.

Hamelin, S., Amyot, M., Barkay, T., Wang, Y.P., Planas, D., 2011. Methanogens: Principal methylators of mercury in lake periphyton. Environ. Sci. Technol. 45, 7693–7700.

Hammerschmidt, C.R., Fitzgerald, W.F., 2006. Methylmercury cycling in sediments on the continental shelf of southern New England. Geochim. Cosmochim. Acta 70, 918–930.

Hu, H.Y., Lin, H., Zheng, W., Rao, B., Feng, X.B., Liang, L.Y., Elias, D.A., Gu, B.H., 2013. Mercury reduction and cell-surface adsorption by *Geobacter sulfurreducens* PCA. Environ. Sci. Technol. 47, 10922–10930.

Jonsson, S., Skyllberg, U., Nilsson, M.B., Westlund, P.O., Shchukarev, A., Lundberg, E., Bjorn, E., 2012. Mercury methylation rates for geochemically relevant Hg-II species in sediments. Environ. Sci. Technol. 46, 11653–11659.

Kronberg, R.M., Schaefer, J.K., Bjorn, E., Skyllberg, U., 2018. Mechanisms of methyl mercury net degradation in alder swamps: the role of methanogens and abiotic processes. Environ. Sci. Technol. Lett. 5, 220–225.

Kronberg, R.-M., Tjerngren, I., Drott, A., Björn, E., Skyllberg, U., 2012. Net degradation of methyl mercury in alder swamps. Environ. Sci. Technol. 46, 13144–13151.

Laine, A.M., Selanpaa, T., Oksanen, J., Sevakivi, M., Tuittila, E.S., 2018. Plant diversity and functional trait composition during mire development. Mires Peat 21.

Lambertsson, L., Nilsson, M., 2006. Organic material: the primary control on mercury methylation and ambient methyl mercury concentrations in estuarine sediments. Environ. Sci. Technol. 40, 1822–1829.

Lambertsson, L., Lundberg, E., Nilsson, M., Frech, W., 2001. Applications of enriched stable isotope tracers in combination with isotope dilution GC-ICP-MS to study mercury species transformation in sea sediments during in situ ethylation and de-termination. J. Anal. At. Spectrom. 16, 1296–1301.

Lehnherr, I., St Louis, V.L., Kirk, J.L., 2012. Methylmercury cycling in high arctic wetland ponds: controls on sedimentary production. Environ. Sci. Technol. 46, 10523–10531.

Liu, J., Wang, Z.C., Zhao, H.Y., Peros, M., Yang, Q.N., Liu, S.S., Li, H.K., Wang, S.Z., Bu, Z.J., 2018. Mercury and arsenic in the surface peat soils of the Changbai Mountains, northeastern China: distribution, environmental controls, sources, and ecological risk assessment. Environ. Sci. Pollut. R. 25, 34595–34609.

Liu, R.H., Wang, Q.C., Lu, X.G., Fang, F.M., Wang, Y., 2003. Distribution and speciation of mercury in the peat bog of Xiaoxing'an Mountain, northeastern China. Environ. Pollut. 124, 39–46.

Loseto, L.L., Siciliano, S.D., Lean, D.R.S., 2004. Methylmercury production in high arctic wetlands. Environ. Toxicol. Chem. 23, 17–23.

Madigan, M., Martinko, J., Bender, K., Buckley, D., Stahl, d., 2015. Brock Biology of Microorganisms, 14th edition. Pearson Education limited, England.

Martin-Doimeadios, R.C.R., Monperrus, M., Krupp, E., Amouroux, D., Donard, O.F.X., 2003. Using speciated isotope dilution with GC-inductively coupled plasma MS to determine and unravel the artificial formation of monomethylmercury in certified reference sediments. Anal. Chem. 75, 3202–3211.

Martin-Doimeadios, R.C., Tessier, E., Amouroux, D., Guyoneaud, R., Duran, R., Caumette, P., Donard, O.F.X., 2004. Mercury methylation/demethylation and volatilization pathways in estuarine sediment slurries using species-specific enriched stable isotopes. Mar. Chem. 90, 107–123.

Mason, R.P., Choi, A.L., Fitzgerald, W.F., Hammerschmidt, C.R., Lamborg, C.H., Soerensen, A.L., Sunderland, E.M., 2012. Mercury biogeochemical cycling in the ocean and policy implications. Environ. Res. 119, 101–117.

Mergler, D., Anderson, H.A., Chan, L.H.M., Mahaffey, K.R., Murray, M., Sakamoto, M., Stern, A.H., 2007. Methylmercury exposure and health effects in humans: a world-wide concern. AMBIO 36, 3–11.

Mitchell, C.P.J., Branfireun, B.A., Kolka, R.K., 2008. Spatial characteristics of net me-thylmercury production hot spots in peatlands. Environ. Sci. Technol. 42, 1010–1016.

Morris, B.E., Henneberger, R., Huber, H., Moissl-Eichinger, C., 2013. Microbial syntrophy: interaction for the common good. FEMS Microbiol. Rev. 37, 384–406.

Oremland, R.S., Culbertson, C.W., Winfrey, M.R., 1991. Methylmercury decomposition in sediments and bacterial cultures – involvement of methanogens and sulfate reducers in oxidative demethylation. Appl. Environ. Microbiol. 57, 130–137.

Ortega, S.H., Catalan, N., Bjorn, E., Grontoft, H., Hilmarsson, T.G., Bertilsson, S., Wu, P.P., Bishop, K., Levanoni, O., Bravo, A.G., 2018. High methylmercury formation in ponds fueled by fresh humic and algal derived organic matter. Limnol. Oceanogr. 63, S44–S53.

Pak, K.R., Bartha, R., 1998. Mercury methylation by interspecies hydrogen and acetate transfer between sulfidogens and methanogens. Appl. Environ. Microbiol. 64, 1987–1990.

Parks, J.M., Johs, A., Podar, M., Bridou, R., Hurt Jr., R.A., Smith, S.D., Tomanicek, S.J., Qian, Y., Brown, S.D., Brandt, C.C., Palumbo, A.V., Smith, J.C., Wall, J.D., Elias, D.A., Liang, L., 2013. The genetic basis for bacterial mercury methylation. Science 339, 1332–1335.

Perez-Rodriguez, M., Margalef, O., Corella, J.P., Saiz-Lopez, A., Pla-Rabes, S., Giralt, S., Cortizas, A.M., 2018. The role of climate: 71 ka of atmospheric mercury deposition in the Southern Hemisphere recorded by Rano Aroi Mire, Easter Island (Chile). Geosciences 8.

Petersson-Grawé, K., Concha, G., Ankarberg, E., 2007. Risk Assessment of Methylmercury in Fish. National Food Administration, Sweden Rapport 10.

Poulin, B.A., Ryan, J.N., Tate, M.T., Krabbenhoft, D.P., Hines, M.E., Barkay, T., Schaefer, J., Aiken, G.R., 2019. Geochemical factors controlling dissolved elemental mercury and methylmercury formation in Alaskan wetlands of varying trophic status. Environ. Sci. Technol. 53, 6203–6213.

Renberg, I., Segerström, U., 1981. The initial points on a shoreline displacement curve for southern Västerbotten, dated by varve-counts of lake sediments. In: Königsson, L.-K., Paabo, K. (Eds.), Florilegium Florins Dedicatum. Striae, Uppsala, pp. 174–176.

Rodriguez-Gonzalez, P., Bouchet, S., Monperrus, M., Tessier, E., Amouroux, D., 2013. In situ experiments for element species-specific environmental reactivity of tin and mercury compounds using isotopic tracers and multiple linear regression. Environ. Sci. Pollut. R. 20, 1269–1280.

Rotaru, A.-E., Shrestha, P.M., Liu, F., Shrestha, M., Shrestha, D., Embree, M., Zengler, K., Wardman, a.Colin, Nevina, K.P., Lovley, D.R., 2014. A new model for electron flow during anaerobic digestion: direct interspecies electron transfer to Methanosaeta for the reduction of carbon dioxide to methane. Environ. Sci. Technol. 7, 408.

State of Michigan, 2016, https://www.michigan.gov/, 2019. Michigan Fish Consumption Advisory Program Guidance Document. Version 4.

Schaefer, J.K., Kronberg, R.M., Morel, F.M.M., Skyllberg, U., 2014. Detection of a key Hg methylation gene, *hgc*A, in wetland soils. Environ. Microbiol. Rep. 6, 441–447.

Selvendiran, P., Driscoll, C.T., Montesdeoca, M.R., Bushey, J.T., 2008. Inputs, storage, and transport of total and methyl mercury in two temperate forest wetlands. J. Geophys. Res. Biogeosci. 113.

Skyllberg, U., Qian, J., Frech, W., Xia, K., Bleam, W.F., 2003. Distribution of mercury, methyl mercury and organic sulphur species in soil, soil solution and stream of a boreal forest catchment. Biogeochemistry 64, 53–76.

St Louis, V.L., Rudd, J.W.M., Kelly, C.A., Bodaly, R.A., Paterson, M.J., Beaty, K.G., Hesslein, R.H., Heyes, A., Majewski, A.R., 2004. The rise and fall of mercury me-thylation in an experimental reservoir. Environ. Sci. Technol. 38, 1348–1358.

StLouis, V.L., Rudd, J.W.M., Kelly, C.A., Beaty, K.G., Flett, R.J., Roulet, N.T., 1996. Production and loss of methylmercury and loss of total mercury from boreal forest catchments containing different types of wetlands. Environ. Sci. Technol. 30, 2719–2729.

Taylor, B.F., Oremland, R.S., 1979. Depletion of adenosine-triphosphate in desulfovibrio by oxyanions of group-vi elements. Curr. Microbiol. 3, 101–103.

Tjerngren, I., Meili, M., Bjorn, E., Skyllberg, U., 2012a. Eight boreal wetlands as sources and sinks for methyl mercury in relation to soil acidity, C/N ratio, and small-scale flooding. Environ. Sci. Technol. 46, 8052–8060.

Tjerngren, I., Karlsson, T., Bjorn, E., Skyllberg, U., 2012b. Potential Hg methylation and MeHg demethylation rates related to the nutrient status of different boreal wetlands. Biogeochemistry 108, 335–350.

Tuittila, E.S., Juutinen, S., Frolking, S., Valiranta, M., Laine, A.M., Miettinen, A., Sevakivi, M.L., Quillet, A., Merila, P., 2013. Wetland chronosequence as a model of peatland development: vegetation succession, peat and carbon accumulation. Holocene 23, 25–35.

UNEP, 2017. Minamata Convention on Mercury (UNEP 2017).

USEPA, 2017. National Listing of Fish Advisories, Fish and Shellfish Advisories and Safe Eating Guidelines. www.epa.gov/choose-fish-and-shellfish-wisely/fish-and-shellfish-advisories-and-safe-eating-guidelines.

Walker, D.J.F., Nevin, K.P., Holmes, D.E., Rotaru, A.-E., Ward, J.E., Woodard, T.L., Zhu, J., Ueki, T., Nonnenmann, Stephen S., McInerney, Michael J., Lovley, D.R., 2018. Syntrophus Conductive Pili Demonstrate That Common Hydrogen-donating Syntrophs Can Have a Direct Electron Transfer Option. bioRxiv, preprint. .

Warner, K.A., Roden, E.E., Bonzongo, J.C., 2003. Microbial mercury transformation in anoxic freshwater sediments under iron-reducing and other electron-accepting con-ditions. Environ. Sci. Technol. 37, 2159–2165.

Wu, W.M., Hickey, R.F., Zeikus, J.G., 1991. Characterization of metabolic performance of methanogenic granules treating brewery waste-water – role of sulfate-reducing bac-teria. Appl. Environ. Microbiol. 57, 3438–3449.

Yu, R.Q., Flanders, J.R., Mack, E.E., Turner, R., Mirza, M.B., Barkay, T., 2012. Contribution of coexisting sulfate and iron reducing bacteria to methylmercury production in freshwater river sediments. Environ. Sci. Technol. 46, 2684–2691.

Yu, R.-Q., Reinfelder, J.R., Hines, M.E., Barkay, T., 2018. Syntrophic pathways for mi-crobial mercury methylation. ISME J. 12, 1826–1835.

Zehnder, A.J.B., Brock, T.D., 1979. Methane formation and methane oxidation by me-thanogenic bacteria. J. Bacteriol. 137, 420–432.